ADVANCED MATERIALS
www.advmat.de

Textile Waste Fiber Regeneration via a Green Chemistry Approach: A Molecular Strategy for Sustainable Fashion

Xuantong Sun, Xi Wang, Fengqiang Sun, Mingwei Tian, Lijun Qu, Patsy Perry, Huw Owens, and Xuqing Liu**

Fast fashion, as a continuously growing part of the textile industry, is widely criticized for its excessive resource use and high generation of textiles. To reduce its environmental impacts, numerous efforts are focused on finding sustainable and eco-friendly approaches to textile recycling. However, waste textiles and fibers are still mainly disposed of in landfills or by incineration after their service life and thereby pollute the natural environment, as there is still no effective strategy to separate natural fibers from chemical fibers. Herein, a green chemistry strategy is developed for the separation and regeneration of waste textiles at the molecular level. Cellulose/wool keratin composite fibers and multicomponent fibers are regenerated from waste textiles via a green chemical process. The strategy attempts to reduce the large amount of waste textiles generated by the fast-developing fashion industry and provide a new source of fibers, which can also address the fossil fuel reserve shortages caused by chemical fiber industries and global food shortages caused by natural fiber production.

1. Introduction

Fast fashion, quickly expanded for its quick turnaround and low prices, has been criticized for ushering throwaway culture into the clothing business, thereby limiting the sustainability of this industry. Every year, 150 billion garments are produced by the fashion industry,[1] of which 30% are never sold and over 50% are disposed of in under a year,[2] leading to an estimated US Dollar 500 billion value loss.[3] Approximately 92 million tons of textile wastes are generated annually around the world,[4] 85% of which ends up in landfills (occupying ≈5% of landfill space) or incinerated (when most of these materials could be reused).[5–7] These numbers grow every year due to increasing overproduction and overconsumption, leading to resource waste, environmental contamination,[8] and potential threats to human health from microfibers found in rivers, oceans and drinking water, which could bioaccumulate via the food chain.[9–15] Despite the high production of textile wastes, their recycling rates remain low: only 15% of textile waste was collected and sorted for recycling in 2015, and 1.1 million tons were lost during the process.[16] Most recycled textiles cascade to other industries and are downcycled into lower-value applications.[17]

To address the environmental concerns and prolong the practical service life of fashion textiles, the concept of sustainable fashion and circular economy was put forward, driven by replacing traditional cycle (fabrication, use and dispose) with reuse and recycling.[18–20] Textile reuse and recycling routes, including both closed-loop and open-loop routes, can be divided theoretically into several steps (**Figure 1**).[21] Garments can be reused by transferring them to new owners through donating, swapping and reselling and, for those obsolescent ones, even upcycling by adding valuable features and remodeling.[22,23] When a garment is no longer suitable for wear, its fabric can be recycled into new products, such as upholstery, low-grade blankets, industrial rags, and insulation materials.[24] Even after a fabric is disassembled, the remaining fibers can be isolated for potential use in carpet padding, thermal insulation, and acoustic sound absorbers.[25–30] However, the ideal closed-loop route, in which materials are infinitely and effectively cycled without further energy consumption and pollution, cannot yet be achieved in practice. As fibers are shortened and degraded in each round of recycling, they have an estimated lifetime of 7–9 (plastic fibers) and 4–6 (cellulose fibers) reuses and recycles,[31,32] after which the textiles will eventually end up in landfills or incinerated, thereby polluting the natural environment.

X. Sun, X. Wang, H. Owens, X. Liu
Department of Materials
The University of Manchester
Manchester M13 9PL, UK
E-mail: xuqing.liu@manchester.ac.uk
F. Sun, M. Tian, L. Qu
Research Center for Intelligent and Wearable Technology
College of Textiles and Clothing
State Key Laboratory of Bio-Fibers and Eco-Textiles
Collaborative Innovation Center for Eco-Textiles of Shandong Province and the Ministry of Education
Intelligent Wearable Engineering Research Center of Qingdao
Qingdao University
Qingdao, Shandong 266071, P.R. China
E-mail: lijunqu@qdu.edu.cn
P. Perry
Manchester Fashion Institute
Manchester Metropolitan University
Manchester M15 6BG, UK
The ORCID identification number(s) for the author(s) of this article can be found under https://doi.org/10.1002/adma.202105174.

DOI: 10.1002/adma.202105174

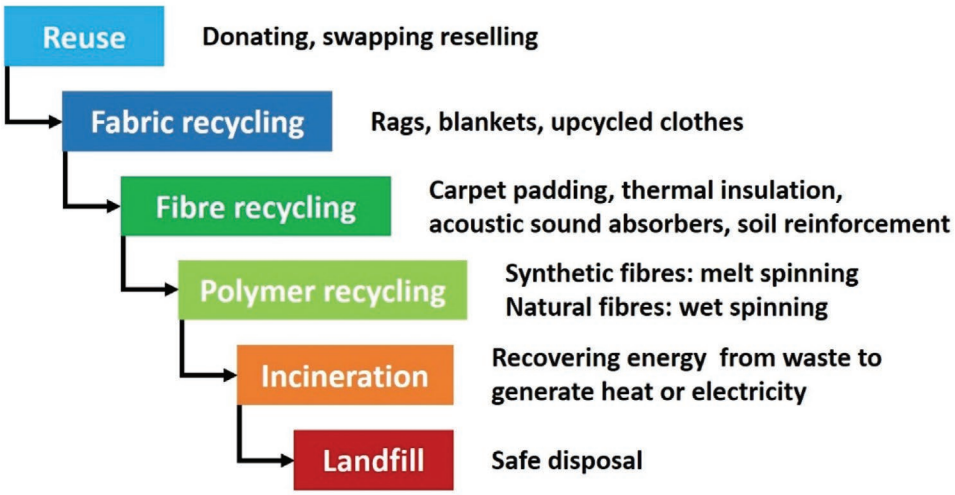

Figure 1. A hierarchical model of the reuse and recycling of textile waste.

Given the current low recycling rates, solving the problem of fashion waste and improving environmental and resource sustainability are left to material scientists. From a material perspective, the current major barrier hindering textile recycling is the lack of technologies for sorting and separation.[21] Most synthetic fibers, such as polyesters, can be reused easily by melt spinning when pure fractions of fibers can be isolated.[33,34] However, most fabrics are generally made by various kinds of fiber blends to produce better performance and improve the texture,[21,35,36] such as cotton/polyester and wool/polyester blends, which makes them difficult or nearly impossible to separate.[37] Despite the labor-intensive and time-consuming sorting process,[38] such blends cannot be simply recycled as a whole by melt spinning since natural fibers are mostly thermoset; therefore, the β-sheet nanocrystallites in the structure would be degraded prior to melting when subjected to thermal processing.[39] Thus, the critical question is how to separate natural fibers from synthetic fibers. Traditional methods for the regeneration of natural fibers usually employ concentrated acidic or alkaline solutions, which destroy the polymer structures of fibers, rendering them unusable as fibers in textiles and fashion. Moreover, these chemical processes unavoidably introduce hazardous substances and have been strictly prohibited in some countries.[40,41] As we cannot cause one environmental problem while solving another, finding a green and sustainable process for waste blended fiber separation will benefit the sustainable development of the fashion industry and reduce pollution, such as that by ubiquitous plastic particles. Hence, ionic liquids (ILs) were chosen to be the solvent for textile wastes separation in this research, which are closely associated with the green chemistry movement because of their low volatility, nonderivatization, and renewability. ILs are capable of dissolving recalcitrant natural biopolymers with massive inter- and intra-molecular hydrogen bonds which cannot be recycled via melt spinning, without producing hazardous byproducts or gas discharge in the reaction.[42–53]

To separate textile materials from general waste, two ILs with different selectivity for polymer dissolution, [BMIM][Cl] and [MMIM][DMP], were selected as green solutions. Both of them have proved the ability to dissolve cellulose and wool,[42,44–48,50–53] of which [BMIM][Cl] shows a wider-ranged selectivity that can dissolve not only natural fibers but also some synthetic ones such as acrylic and nylon.[54,55] But the composition of general waste textiles is complex, including cotton and wool which are also commonly used by blending together thus difficult to separate. To simulate and provide solutions for general textile waste in actual recycling, cotton and wool were dissolved and regenerated together in the weight ratio of cotton:wool = 1:1, which was determined to better reflect their distinctive characteristics in the regenerated mixture. In this research, cotton/polyester and wool/polyester blended fabrics from used garments were utilized for dissolution and regeneration, respectively. After dissolution, the remaining undissolved synthetic polymer could be collected and simply recycled into fiber via the traditional melt spinning process, while the extracted cellulose and wool keratin were regenerated via wet spinning. And the ILs could be recovered and reused constantly by distillation after the regeneration of extracted polymers, thereby achieving the complete closed-loop route for textile recycling.

It's also worth mentioning that the regenerated cellulose/wool keratin composite fiber wet-spun from [MMIM][DMP] exhibits a unique morphology, with wool keratin microspheres adhered on the surface, that is different from the morphologies reported in previous studies,[56–58] and outstanding moisture absorption capacity which can provide good comfort for wearing. This research also provides a green and sustainable option for large-scaled textile waste recycling to the fashion industry.

2. Results and Discussion

Blended cotton/polyester (50%/50%) and wool/polyester (50%/50%) fabrics from used garments were separated by dissolution with ILs, leaving undissolved polyester fibers to treat via melt spinning. [BMIM][Cl] and [MMIM][DMP] were applied relatively to evaluate the dissolution process, and three different ratios (cotton/polyester:wool/polyester = 1:0, 1:1, 0:1) of

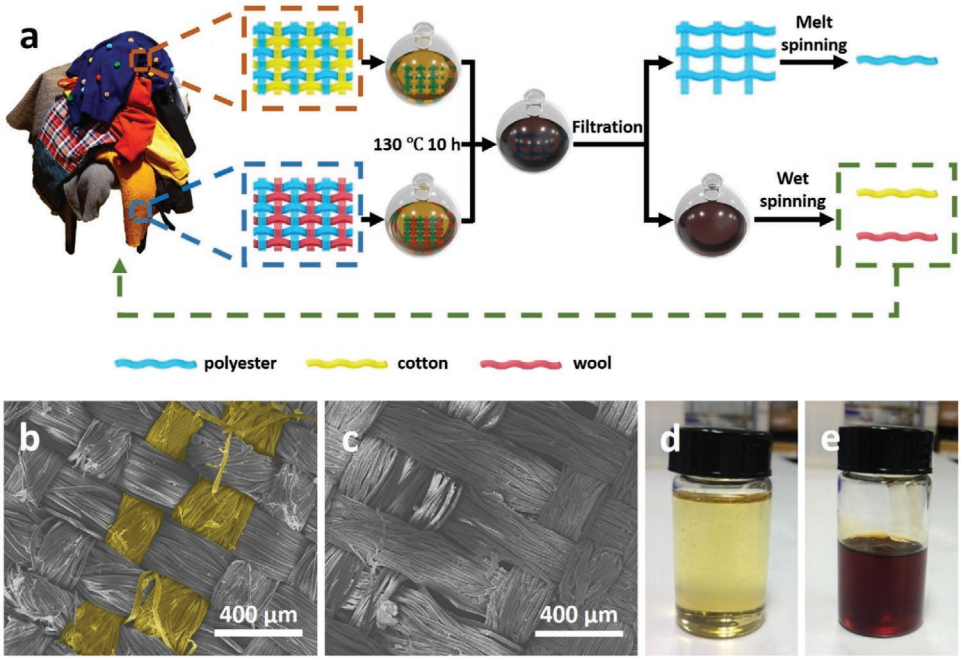

Figure 2. Performance of ionic liquids in the separation of natural polymers from polyester composite blended fabrics. a) A schematic diagram of the separation and regeneration of cotton/polyester blended fabric. b) SEM image of cotton/polyester blended fabric before dissolution. c) SEM image of the polyester fabric remaining after dissolution. d) Photograph of the [BMIM][Cl] ionic liquid. e) Photograph of cellulose and wool keratin dissolved in the [BMIM][Cl] ionic liquid.

the blended fabrics were applied in the experiment (**Figure 2**a). The waste pure acrylic fabric was also investigated for solubility in these two ILs in the same experimental condition, which turns out can only be dissolved in [BMIM][Cl]. As illustrated in Figure 2b,c, the surface of the blended weaving fabric had a hair-like structure arising from the cotton fibers aligned in the weft direction; this structure was disrupted by dissolution, whereas the smooth polyester fibers aligned in the warp direction remained unchanged. During dissolution, the color of [BMIM][Cl] turned from clear yellow to dark brown (Figure 2d,e).

After dissolution, all solutions of IL with extracted polymers (cellulose-[BMIM][Cl], acrylic-[BMIM][Cl], wool keratin-[MMIM][DMP], cellulose/wool keratin-[MMIM][[DMP], etc.) were first tried to be regenerated into fiber via wet spinning, through which only cellulose from both ILs, cellulose/wool keratin composite from [MMIM][DMP] and acrylic from [BMIM][Cl] were successfully obtained (of which the regenerated acrylic fiber will become brittle after dried, thereby cannot be directly used as fiber for textile manufacture). Alternatively, wool keratin from both ILs and cellulose/wool keratin composite from [BMIM][Cl] were regenerated into hydrogel films.

To analyze the chemical changes occurring during the dissolution and regeneration, ATR-FTIR spectroscopy of native polymer fabrics, regenerated cellulose, wool keratin, cellulose/keratin composite and acrylic materials was carried out, as illustrated in **Figure 3**a–c,g. To understand the crystallinity structures and polymorphy of the native and regenerated polymer samples, X-ray diffraction measurements were employed, and the diffractograms are compared in Figure 3d–f,h.

The spectrum of the regenerated cellulose is similar to that of the cotton fabric: no new peaks were detected. This indicates that cellulose was recovered from the IL without distinct chemical structure changes. The broad band at 3326 cm^{-1} is assigned to the stretching of —OH groups, which indicates the presence of hydrogen bonds. The signal at ≈2890 cm^{-1} could correspond to C—H stretching, and the band at 1645 cm^{-1} is attributed to amorphous water. The peak at 1316 cm^{-1} originated from O—H bending vibrations, and the small sharp band at 899 cm^{-1} could be due to O—H stretching. The strong band at ≈1011 cm^{-1} is assigned to the characteristic C—O—C stretching, the intensity of which is weaker than that in the spectrum of the raw cotton fabric. The crystalline structures of cellulose can be divided into six polymorphic forms (cellulose I, II, III_I, III_{II}, IV_I, and IV_{II}), of which cellulose I is the form in nature and can be converted into the more stable cellulose II, with a 3D network structure, via regeneration or mercerization.[59,60] The diffractogram (XRD) of the cotton fabric exhibits the typical pattern of cellulose |, with peaks at ≈14.87°, 16.62°, 22.78°, and 34.52°, representing crystallographic planes (10), (110), (220), and (004).[60] The patterns of the regenerated cellulose from the ILs show peaks at 2θ = 12.02°, 20.00°, 21.70°, and 34.52°, representing crystallographic planes (10), (110), (020), and (004), corresponding to cellulose ||.[61] These results indicate the transformation from cellulose | to cellulose ||, with rapid breaking and reforming of inter- and intra-molecular hydrogen bonds among cellulose molecules during the process.[62] Moreover, the lower- and borderline-crystallinity peaks of regenerated cellulose reflect a decrease in crystallinity, probably due to a coagulation process that is unfavorable to cellulose crystallization.[63]

The spectra of the wool fabric and regenerated wool keratin show almost identical characteristic absorption bands that

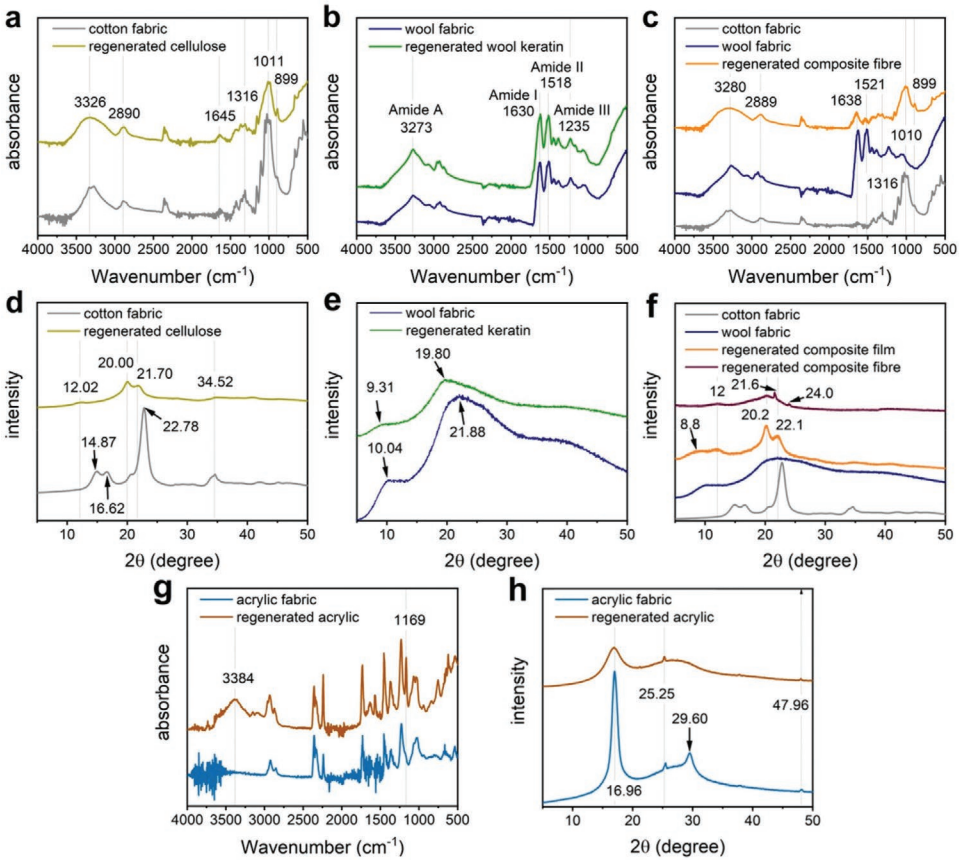

Figure 3. Characterization of the regenerated polymer materials. FTIR spectra of a) cotton and regenerated cellulose, b) wool and regenerated wool keratin, and c) cotton, wool, and regenerated cellulose/wool keratin composite. XRD patterns of d) cotton and regenerated cellulose, e) wool and regenerated wool keratin, and f) regenerated cellulose, wool, and regenerated cellulose/wool keratin composite. g) FTIR spectra and h) XRD patterns of acrylic and regenerated acrylic.

could be traced back to peptide bonds (−CONH), suggesting the successful recovery of wool keratin. The absorption band at 3273 cm^{-1} could be due to N−H stretching from amide A vibrations. The strong peak observed at 1630 cm^{-1} corresponds to C=O in the amide | band, and the peak at 1518 cm^{-1} is from N−H bending and C−N stretching in amide ||. A weak band at 1235 cm^{-1} is assigned to C−O and C−N stretching and O=C−N and N−H bending in amide III. Two typical crystal structures are determined from the diffractogram of raw wool fabric, with a peak at ≈10.04° attributed to an α-helix structure and a peak at 21.88° indicating a β-sheet structure.[64] The XRD diffractogram of the regenerated wool keratin generally matches that of the raw wool fabric except that the peaks are significantly weaker, indicating lower crystallinity and a more amorphous structure, which can improve water absorption.

In the spectrum of the regenerated cellulose/wool keratin composite, the peaks corresponding to amide | and amide II are at ≈1638 and 1521 cm^{-1}, but their intensities are lower than those above due to the decreased concentration of keratin in the blend.[65] The peaks at 1010 and 899 cm^{-1} are consistent with those in the cotton fabric. Similar to that of the regenerated cellulose, the XRD diffractogram of the regenerated cellulose/wool keratin film contains peaks at 20.02° and 21.83°, indicating that the cellulose II structure is present in the composite, and the peaks at 8.89° and 12.07° could be a result of the presence of wool keratin. The small and sharp peaks at 21.59° and 24.00° in the regenerated composite fiber are probably a result of the β-sheet structure from wool keratin and the cellulose II structure from cellulose. No new peaks appear in the FTIR spectrum of the regenerated composite in comparison with the spectra of regenerated pure cellulose and wool keratin, indicating that the macromolecular structure remains unchanged during the dissolution and regeneration; instead, bonds in the crystal structure break, resulting in polymer chain rearrangement.

The ATR spectrum of regenerated acrylic is similar to that of the raw fabric, except that it contains peaks at 3384 and 1169 cm^{-1}, which may correspond to the stretching of −OH groups and C−N stretching, respectively. Compared to the XRD diffractogram of the original acrylic, in the diffractogram of the regenerated acrylic, the major crystallinity peak at 16.96° is much weaker, and the peak at 29.60° is absent, which indicates that the acrylic became amorphous and the crystal structure was damaged during recycling.

The regeneration of dissolved natural polymers can be achieved by diffusional interchange between the IL and a liquid bath, which is also known as the coagulation step of the wet-spinning process. Here, water was chosen for the coagulation bath, in which cellulose fiber and cellulose/wool keratin composite fiber were regenerated, and their SEM images are shown in **Figure 4**a–i; Figure S5a–i, Supporting Information. As

shown in Figure 4a–c, the regenerated cellulose fiber exhibits a smooth and even surface with a streaky appearance, of which the fibrillar texture was formed by the polymer chains of D-glucose units lying alongside each other.[66] Despite the consistency of the regenerated cellulose fiber morphology with that reported in previous studies,[56] it is interesting that the morphology of the regenerated cellulose/wool keratin composite fiber illustrated in Figure 4d–i is significantly different from that reported in previous studies.[56–58] Two types of cellulose/wool keratin composite fibers with the same blend ratio of 2.5 wt%/2.5 wt% were obtained via wet spinning from [MMIM][DMP], presenting a similar fiber diameter but distinct morphology as a result of the different spinning speeds. The morphology of the composite fiber regenerated at a lower spinning speed is demonstrated in Figure 4d–f; Figure S5a–c, Supporting Information, showing tightly packed globular microparticles covering the surface, while the fiber spun at a higher spinning speed, shown in Figure 4g–i; Figure S5d–i, Supporting Information, exhibits a fibril structure along the spinning direction and "globules" growing from the gaps. Both types of fibers display a phase-separated structure. Referring to previous studies, we found a similar globular structure in regenerated wool keratin particles and silk fibers,[39,67–72] thus indicating that the microspheres on the surface of the composite fibers are polymeric micelles self-assembled by wool keratin and the fibril structure was formed by cellulose (Figure 4j).

This unique morphology may be explained by the amphiphilicity of wool keratin and the rearrangement of its chain folding. During dissolution, the breaking of disulfide bridges and hydrogen bonds is oriented by [MMIM][DMP], leading to the disruption of the 3D structure of wool keratin and the unfolding of the α-helix. The disappearance of the coiled–coil architecture of α-helix can be confirmed by Raman spectroscopy and SAXS profile. As illustrated in Figure 4l, instead of the typical peak corresponding to keratin α-helix structure commonly observed ≈0.1 nm^{-1} in previous studies,[73,74] the SAXS profile of the regenerated cellulose/wool keratin composite fiber exhibits a board shoulder, indicating the presence of molecular organizations formed within amorphous structure, consistent with the XRD results in Figure 3.[75,76] And characteristic bonds belonging to α-helix at 928, 1271, and 1652 cm^{-1} are absent in the Raman spectroscopy shown in Figure 4m; alternatively, a peak at 1247 cm^{-1} can be observed, suggesting a disordered amino III structure.[74,77]

The resultant amorphous polypeptide chains are amphiphilic, consisting of both hydrophobic and hydrophilic amino acids with their side chains extending outward, potentially enabling the formation of micelles in water. The amphiphilicity of polypeptide chains can be verified by the result of surface tension measurement (Figure 4k), as the surface tension of water became lower after the addition of 3 mL mixture of [MMIM][DMP] with 5 wt% cellulose/wool keratin (1:1) compared to only adding 3 mL [MMIM][DMP], implying a further decrease of surface tension was induced by the formation of amphiphilic polypeptide chains. The main driving force for micelle formation, a thermodynamic process, is the minimization of the interfacial free energy of the polymer–water system.[78] When the spinning dope of dissolved polymers is added to water, the polymer concentration rapidly increases and reaches the critical micelle concentration (CMC), thus inducing the self-assembly

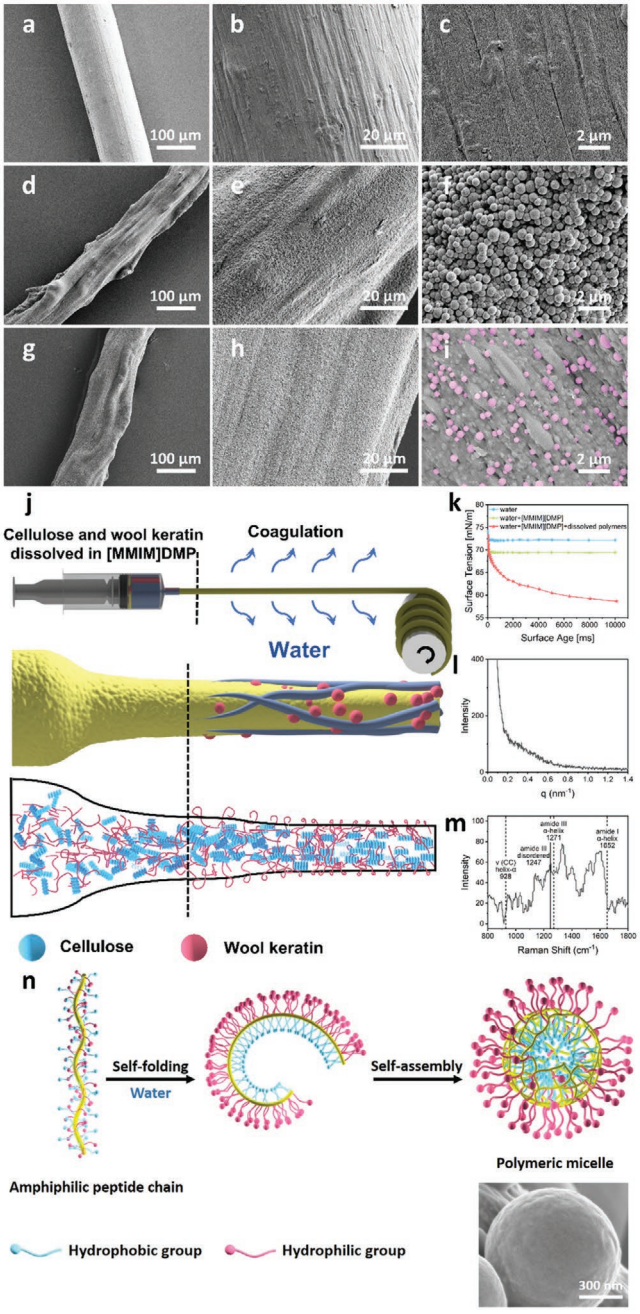

Figure 4. Morphology of the regenerated polymer fibers. a–c) SEM images of regenerated cellulose fiber. d–f) SEM images of cellulose/wool keratin (w/w = 1/1) composite fiber regenerated via [MMIM][DMP] at a lower spinning speed during the wet-spinning process. g–i) SEM images of cellulose/wool keratin (w/w = 1/1) composite fibers regenerated via [MMIM][DMP] at a higher spinning speed during the wet-spinning process. j) Schematic of the formation of the morphology of regenerated cellulose/wool keratin composite fiber. k) Surface tension measurement of distilled water (25 mL), 25 mL water with addition of 3 mL [MMIM][DMP], and 25 mL water with addition of 3 mL mixture of 5 wt% cellulose/wool keratin (1:1) dissolved in [MMIM][DMP]. l) SAXS profile of the regenerated cellulose/wool keratin composite fiber. m) Raman spectroscopy of the regenerated cellulose/wool keratin composite fiber. n) Self-assembly model including chain folding and micelle formation of wool keratin.

of wool keratin. As illustrated in Figure 4n, the polypeptide chains tend to coil and aggregate once spun into the water and eventually self-assemble into a spherical structure, with the main chains bound to each other through intermolecular disulfide bonds. The R-groups from hydrophobic amino acids (such as Cys, Leu, Pro, and Gly) clump into the center to form the core, while the polar groups from hydrophilic amino acids (such as Glu, Ser, and Arg) shield the inside from contact with water, thereby reducing the interfacial free energy to attain the most stable state (Figure S6, Supporting Information). Meanwhile, cellulose, as an unbranched molecule, is regenerated from randomly oriented D-glucose subunits back to aligned polymeric chains along the spinning direction, which make up the fibril structure on the fiber surface.

The effect of the spinning conditions on micelle formation have also been demonstrated. As shown in Figure S5a–c, Supporting Information, the regenerated cellulose/wool keratin fiber obtained via a lower spinning speed presents obviously more "globules" on its surface, which suggests that the number of distributed micelles can be controlled by the duration of the contact with water. In addition, we observed that the sizes of micelles from different parts of the same fiber differ, as the diameters of the "globules" on the anterior part of the fiber obtained at a higher spinning speed (Figure S5d–f, Supporting Information) vary from 140–600 nm, similar to the fiber obtained at the lower speed, while the sizes of the "globules" on the posterior part (Figure S5g–i, Supporting Information) range between 100 and 300 nm. This could be explained by the principle of the wet-spinning process and the properties of ILs, as the filament is formed by diffusional interchange with coagulation.[79] When ILs diffuse into water, the surface tension of the water will be reduced by the addition of this surfactant, restraining the diffusional interchange, thus limiting further formation of keratin micelles.

To verify the potential of regenerated fibers for practical application in textile industry, their mechanical properties and moisture absorption capability were investigated, and the results are shown in **Figure 5**a–f. Overall, the regenerated

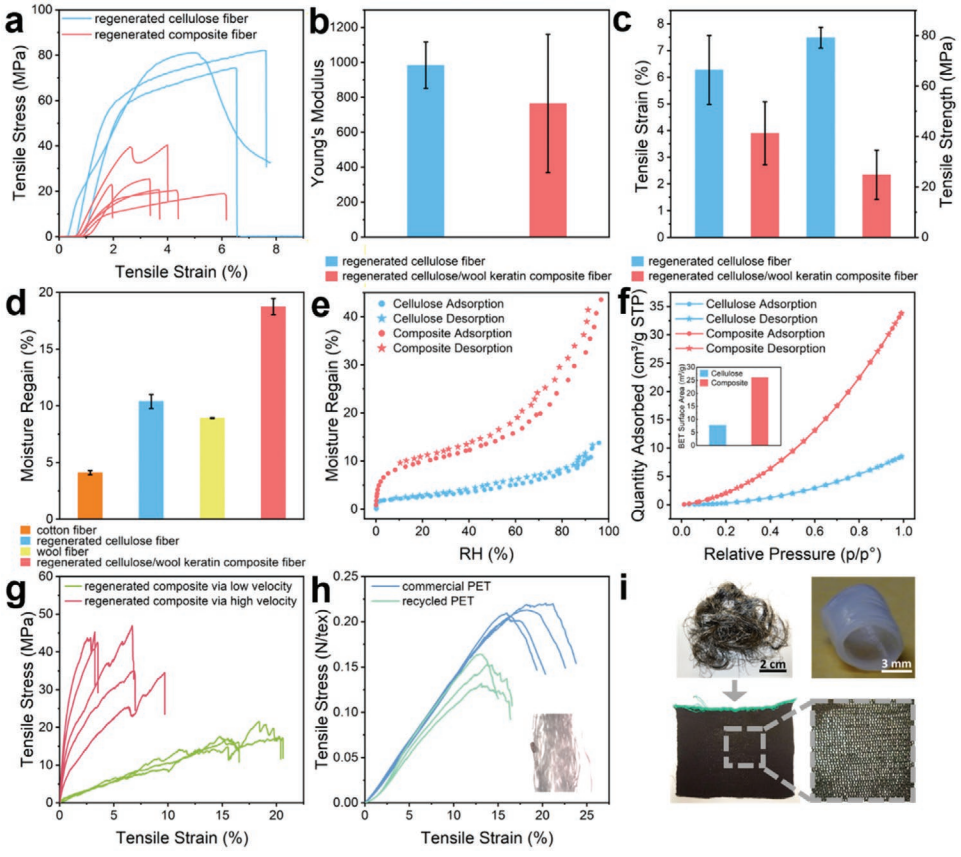

Figure 5. Mechanical properties of the regenerated polymer materials. a) Respective stress–strain curves of the regenerated cellulose fiber and cellulose/wool keratin composite fiber. b) Young's modulus of the regenerated cellulose fiber and cellulose/wool keratin composite fiber. c) Tensile strain and strength at maximum load of the regenerated cellulose fiber and cellulose/wool keratin composite fiber. d) Moisture regain rate of cotton, wool, regenerated cellulose, and regenerated cellulose/wool keratin composite fibers for 24 h at 20 °C and 25% relative humidity. e) The equilibrium moisture regain of regenerated cellulose fiber and regenerated cellulose/wool keratin composite fiber. The sorption/desorption cycles were measured at a temperature of 25 °C. f) Nitrogen adsorption–desorption isotherms of regenerated cellulose fiber and regenerated cellulose/wool keratin composite fiber. The inset refers to the BET surface area analysis. g) Respective stress–strain curves of the regenerated cellulose/wool keratin composite fibers via relatively lower and higher spinning speed. h) Respective stress–strain curves of commercial polyester fiber and recycled polyester fiber by melt spinning. The inset refers to the optical microscopy image of recycle polyester fiber. i) Photos of the regenerated cellulose/wool keratin composite fiber via [MMIM][DMP] (top left), a piece of fabric manufactured from the regenerated composite fiber via double stranded knitting (below), and the regenerated cellulose/wool keratin hydrogel via [BMIM][Cl] (top right).

cellulose fiber exhibits relatively better mechanical property compared to regenerated cellulose/wool keratin fiber, consistent with previous studies which suggest the addition of cellulose may enhance the poor mechanical strength of wool keratin.[56,65,80] However, the distinction of mechanical properties between these two regenerated fibers isn't that significant, and both of them have shown much weaker physical properties than virgin commercial cotton or wool fibers, which might have resulted from the decrease of crystallinities after regeneration. We have also tried to manufacture the regenerated cellulose/wool keratin composite fiber into a small piece of fabric, and successfully achieve it via double-strand knitting (Figure 5i). Since the mechanical property of the composite fiber is weaker between these two regenerated fibers, their potential for practical use in textile manufacturing has been verified.

Two measurements were conducted to investigate the moisture adsorption capability of the regenerated fibers, of which one is the moisture regain in an environment of 20 °C and 25% relative humidity for 24 h in comparison with commercial fibers shown in Figure 5d, and the other is water vapor sorption of the regenerated fibers at 25 °C illustrated in Figure 5e. In comparison with commercial cotton and wool fibers, both the regenerated fibers show better moisture regain properties, indicating good comfortability for wearing.[81] The general good moisture regain properties of the regenerated fibers could possibly be due to their low crystallization rate and free volume inside, supported by XRD results in Figure 3. Notably, the moisture regain rate of regenerated cellulose/wool keratin fiber is distinctly outstanding, which might also benefit from the increased surface area (Figure 5f) as the result of its unique morphology.

Considering that the morphology of regenerated cellulose/wool keratin composite fiber would be influenced by the spinning speed during wet spinning process, the effect of different velocities on their mechanical properties was further investigated. To observe the result difference more clearly, we choose two distinct spinning speeds, one of which is close to zero and the other is approaching the up limit for stable spinning. As the feeding rate from spinneret remains the same in the experiment, the composite fiber regenerated via lower spinning speed exhibits slightly curly appearance due to the resultant low spinneret draft ratio, and thus exhibits better tensile strain result. In contrast, the fiber regenerated by higher spinning speed shows better tensile strength and lower tensile strain. Restricted by experimental conditions, the higher velocity of spinning cannot be kept very constant, for which the fiber regenerated via higher spinning speed shows more varied results of mechanical properties.

To provide a full picture of the circular route for textile waste recycling, we have also tried to recycle the remaining polyester left behind from the separation process. The polyester was completely washed and dried after dissolution to remove any impurity, and then recycled via melt spinning. As illustrated in Figure 5h, the recycled polyester fiber exhibits similar mechanical property compared to new commercial polyester fiber, but a little bit weaker. The possible reason could be the abrasion during wearing and residual impurity from incomplete separation (Figure 5h inset). And this strength loss can be improved by mixing with virgin fiber or PET bottles when applied in industrial textile recycling.[38,82] However, the mechanical properties of the regenerated fibres could be optimized by the spinning and drawing process.

In addition to fibers, we demonstrated the application of other regenerated cellulose/wool keratin composite product in the form of cyclic annular hydrogels (Figure 5i), further application and modification of which will be investigated in future.

3. Conclusion

In this study, a simple method was applied to convert waste textiles into regenerated materials. We utilized two ILs, [BMIM][Cl] and [MMIM][DMP], to separate natural fiber/polyester blended fabrics, which achieves not only blended-fabric separation, providing a feasible method of textile recycling at scale, but also a circular route for complete recycling of waste textiles and cyclic utilization of solvents. Two types of blended fabrics from used garments, cotton/polyester and wool/polyester blends were first separated by the ILs, with cotton and wool dissolved into ILs. The undissolved solid polyester could be simply recycled by traditional melt spinning, while the extracted cellulose and wool keratin could be regenerated via wet spinning.

Several types of natural polymeric products were successfully regenerated from these two ILs using water for coagulation, including regenerated cellulose microspheres, cellulose fiber, freeze-dried wool keratin hydrogel, and cellulose/wool keratin composite hydrogel and fibers, which indicate different suitability of the ILs for practical textile recycling process. We also used [BMIM][Cl] to dissolve and regenerate waste acrylic fabric into fiber, which became brittle after drying and will need further study for application. Cellulose/wool keratin composite fibers were successfully regenerated via [MMIM][DMP] and presented a significantly different morphology from that in previous reports. Microspheres were clearly observed adhered on the surface along the direction of injection, which could indicate a wool keratin component in the mixture. Such regenerated composite fibers showed excellent water vapor adsorption capability and suitable mechanical properties for textile manufacture, supporting their wearability. Our work gives a solution for the critical problem of separating natural and synthetic fibers from waste textiles and represents an emerging breakthrough in fiber material regeneration in a green chemical approach. In future research, more modifications of the regenerated products for functional applications, high-efficient methods for pigment removal from waste textiles, and enhancement of the efficiency and repeatability of ionic liquids recovery after regeneration will be investigated.

Supporting Information

Supporting Information is available from the Wiley Online Library or from the author.

Acknowledgements

This research was supported by the Henry Royce Institute for Advanced Materials, funded through EPSRC grants EP/R00661X/1, EP/P025021/1, and EP/P025498/1.

Note: The spelling of author name Huw Owens was corrected in the author byline and affiliations on November 30, 2021, after initial publication online.

Conflict of Interest

The authors declare no conflict of interest.

Data Availability Statement

The data that supports the findings of this study are available in the supplementary material of this article.

Keywords

sustainable fashion, fiber regeneration, green chemistry, ionic liquids

Received: July 6, 2021
Revised: August 15, 2021
Published online: September 24, 2021

[1] E. Farra, 5 Ways to Make Better and More Sustainable Shopping Decisions – Earth Day, Vogue | Vogue, https://www.vogue.com/article/fast-fashion-environmental-impact-sustainability-parsons-zady (accessed: Aug, 2021).
[2] H. Matevosyan, Overproduction: Taboo in Fashion, https://www.linkedin.com/pulse/overproduction-taboo-fashion-hasmik-matevosyan, (accessed: Aug, 2021).
[3] E. MacArthur, Foundation Circular Fashion – A New Textiles Economy: Redesigning fashion's future, https://ellenmacarthurfoundation.org/a-new-textiles-economy, (accessed: Aug, 2021).
[4] J. Kerr, J. Landry, Pulse of the Industry – GLOBAL FASHION AGENDA, https://www.globalfashionagenda.com/publications-and-policy/pulse-of-the-industry/#, (accessed: Aug, 2021).
[5] E. Humes, *Nature* **2019**, *575*, 278.
[6] Recycle Shoes and Clothing | Textile Recycling Programs, https://worldwearproject.com/global-responsibility/, (accessed: Aug, 2021).
[7] L. J. R. Nunes, R. Godina, J. C. O. Matias, J. P. S. Catalão, *J. Cleaner Prod.* **2018**, *171*, 1353.
[8] The price of fast fashion. *Nat. Clim. Change* **2018**, *8*, 1.
[9] A. Zabala, *Nat. Sustain.* **2018**, *1*, 213.
[10] M. L. Taylor, C. Gwinnett, L. F. Robinson, L. C. Woodall, *Sci. Rep.* **2016**, *6*, 33997.
[11] W. W. Y. Lau, Y. Shiran, R. M. Bailey, E. Cook, M. R. Stuchtey, J. Koskella, C. A. Velis, L. Godfrey, J. Boucher, M. B. Murphy, R. C. Thompson, E. Jankowska, A. C. Castillo, T. D. Pilditch, B. Dixon, L. Koerselman, E. Kosior, E. Favoino, J. Gutberlet, S. Baulch, M. E. Atreya, D. Fischer, K. K. He, M. M. Petit, U. R. Sumaila, E. Neil, M. V. Bernhofen, K. Lawrence, J. E. Palardy, *Science* **2020**, *369*, 1455.
[12] T. W. Walker, N. Frelka, Z. Shen, A. K. Chew, J. Banick, S. Grey, M. S. Kim, J. A. Dumesic, R. C. Van Lehn, G. W. Huber, *Sci. Adv.* **2020**, *6*, eaba7599.
[13] I. Peeken, S. Primpke, B. Beyer, J. Gütermann, C. Katlein, T. Krumpen, M. Bergmann, L. Hehemann, G. Gerdts, *Nat. Commun.* **2018**, *9*, 1505.
[14] D. M. Mitrano, W. Wohlleben, *Nat. Commun.* **2020**, *11*, 5324.
[15] J. R. Jambeck, R. Geyer, C. Wilcox, T. R. Siegler, M. Perryman, A. Andrady, R. Narayan, K. L. Law, *Science* **2015**, *347*, 768.
[16] K. Niinimäki, G. Peters, H. Dahlbo, P. Perry, T. Rissanen, A. Gwilt, *Nat. Rev. Earth Environ.* **2020**, *1*, 189.
[17] E. MacArthur, E. Foundation, The New Plastics Economy: Rethinking the Future of Plastics & Catalysing Action, https://ellenmacarthurfoundation.org/the-new-plastics-economy-rethinking-the-future-of-plastics-and-catalysing, (accessed: Aug, 2021).
[18] X. Chen, H. A. Memon, Y. Wang, I. Marriam, M. Tebyetekerwa, *Mater. Circ. Econ.* **2021**, *3*, 12.
[19] T. Domenech, Explainer: What is a Circular Economy?, https://theconversation.com/explainer-what-is-a-circular-economy-29666, (accessed: Aug, 2021).
[20] P. Manickam, G. Duraisamy, in *Circular Economy in Textiles and Apparel: Processing, Manufacturing, and Design* (Ed: S. S. Muthu), Elsevier, Amsterdam, the Netherlands **2019**, pp. 77.
[21] G. Sandin, G. M. Peters, *J. Cleaner Prod.* **2018**, *184*, 353.
[22] L. M. Fortuna, V. Diyamandoglu, *Waste Manage.* **2020**, *66*, 178.
[23] P. Pandit, G. T. Nadathur, S. Jose, *Upcycled and Low-Cost Sustainable Business for Value-Added Textiles and Fashion*, Elsevier, Amsterdam, the Netherlands **2019**.
[24] P. B. P. Anders Schmidt, D. Watson, S. Roos, C. Askham, *Gaining Benefits from Discarded Textiles*, Nordic Council Of Ministers, Denmark **2016**.
[25] A. Briga-sá, D. Nascimento, N. Teixeira, J. Pinto, F. Caldeira, H. Varum, A. Paiva, *Constr. Build. Mater.* **2013**, *38*, 155.
[26] H.-W. Borger, K. Peter, Heinz-werner (Bobingen, DE), Knobloch, Peter (Grossaitingen), US5723209A, 1998.
[27] D. Trajković, S. Jordeva, E. Tomovska, K. Zafirova, Polyester Apparel Cutting Waste as Insulation Material, *J. Text. Inst.* **2016**, *108*, 1238.
[28] C. Lacoste, R. El Hage, A. Bergeret, S. Corn, P. Lacroix, *Carbohydr. Polym.* **2018**, *184*, 1.
[29] N. M. Aly, H. S. Seddeq, K. Elnagar, T. Hamouda, *J. Build. Eng.* **2021**, *40*, 102747.
[30] J. O. Yeon, K. W. Kim, K. S. Yang, J. M. Kim, M. J. Kim, *Constr. Build. Mater.* **2014**, *70*, 494.
[31] C. A. Echeverria, W. Handoko, F. Pahlevani, V. Sahajwalla, *J. Cleaner Prod.* **2019**, *208*, 1524.
[32] Greener Way to Recycle Clothes Passes with Flying Colours, https://www.nature.com/articles/d42473-019-00359-2 (accessed: Aug, 2021).
[33] N. E. Zander, M. Gillan, Z. Burckhard, F. Gardea, *Addit. Manuf.* **2019**, *25*, 122.
[34] R. Shanks, 5 - Recycled Synthetic Polymer Fibers in Composites. *Green Composites*, Vol. 2, Composites Science and Engineering, Woodhead Publishing, Cambridge, UK **2017**, pp. 73–93.
[35] Textile School, Blended Fabrics, https://www.textileschool.com/265/blended-fabrics-textile-composites/, (accessed: Aug, 2021).
[36] S. Kumar, Polyester Fibre – Uses And Its Blending Property, https://style2designer.com/apparel/fabrics/polyester-fibre-uses-and-its-blending-property/, (accessed: Aug, 2021).
[37] H.&M.'s Green Machine: A recycling solution? | Vogue Business, https://www.voguebusiness.com/sustainability/handms-green-machine-a-recycling-solution, (accessed: Aug, 2021).
[38] A. Beall, Why Clothes are so Hard to Recycle – BBC Future, https://www.bbc.com/future/article/20200710-why-clothes-are-so-hard-to-recycle, (accessed: Aug, 2021).
[39] C. Guo, C. Li, H. V. Vu, P. Hanna, A. Lechtig, Y. Qiu, X. Mu, S. Ling, A. Nazarian, S. J. Lin, D. L. Kaplan, *Nat. Mater.* **2020**, *19*, 102.
[40] S. Wang, A. Lu, L. Zhang, *Prog. Polym. Sci.* **2016**, *53*, 169.
[41] J. Chen, K. Vongsanga, X. Wang, N. Byrne, What Happens during Natural Protein Fibre Dissolution in Ionic Liquids. *Mater.* **2014**, *7*, 6158.
[42] D. L. Minnick, R. A. Flores, M. R. DeStefano, A. M. Scurto, *J. Phys. Chem. B* **2016**, *120*, 7906.
[43] X. Tan, X. Li, L. Chen, F. Xie, *Phys. Chem. Chem. Phys.* **2016**, *18*, 27584.
[44] Y. Ma, L. Rosson, X. Wang, N. Byrne, *J. Text. Inst.* **2020**, *111*, 630.
[45] Y. Cheng, X. Zhang, C. Yin, J. J. Zhang, J. Yu, J. J. Zhang, *Macromol. Rapid Commun.* **2021**, *42*, 2000494.
[46] R. P. Swatloski, S. K. Spear, J. D. Holbrey, R. D. Rogers, *J. Am. Chem. Soc.* **2002**, *124*, 4974.
[47] K. A. Le, C. Rudaz, T. Budtova, *Carbohydr. Polym.* **2014**, *105*, 237.

[48] O. A. El Seoud, A. Koschella, L. C. Fidale, S. Dorn, T. Heinze, *Biomacromolecules* **2007**, *8*, 2629.
[49] Z. Jiang, J. Yuan, P. Wang, X. Fan, J. Xu, Q. Wang, L. Zhang, *Int. J. Biol. Macromol.* **2018**, *119*, 423.
[50] S. Zheng, Y. Nie, S. Zhang, X. Zhang, L. Wang, *ACS Sustainable Chem. Eng.* **2015**, *3*, 2925.
[51] J. Zhang, J. Wu, J. Yu, X. Zhang, J. He, J. Zhang, *Mater. Chem. Front.* **2017**, *1*, 1273.
[52] R. De Silva, X. Wang, N. Byrne, *RSC Adv.* **2014**, *4*, 29094.
[53] R. De Silva, K. Vongsanga, X. Wang, N. Byrne, *Carbohydr. Polym.* **2015**, *121*, 382.
[54] E. Evans, S. Egharevba, Applications of Ionic Liquids in Plastic and Lignin Waste Recycling, *Sustainable Bioconversion of Waste to Value Added Products*, Advances in Science, Technology & Innovation, Springer, Cham , **2021**, pp. 329–336.
[55] S. Wan, Y. Zhang, H. Wang, *Polym. Adv. Technol.* **2009**, *20*, 857.
[56] R. De Silva, X. Wang, N. Byrne, *Carbohydr. Polym.* **2016**, *153*, 115.
[57] K. Kammiovirta, A.-S. Jääskeläinen, L. Kuutti, U. Holopainen-Mantila, A. Paananen, A. Suurnäkki, H. Orelma, *RSC Adv.* **2016**, *6*, 88797.
[58] L. Lucia, A. Ayoub, *Polysaccharide-Based Fibers and Composites*, Springer Nature, Basingstoke, UK **2018**.
[59] A. C. O'Sullivan, *Cellulose* **1997**, *4*, 173.
[60] Z. Liu, X. Sun, M. Hao, C. Huang, Z. Xue, T. Mu, *Carbohydr. Polym.* **2015**, *117*, 54.
[61] S. Nomura, Y. Kugo, T. Erata, *Cellulose* **2020**, *27*, 3553.
[62] H.-Z. Chen, N. Wang, L.-Y. Liu, *J. Chem. Technol. Biotechnol.* **2012**, *87*, 1634.
[63] H. Zhang, J. Wu, J. Zhang, J. He, H. Zhang, J. Wu, J. Zhang, J. He, *Macromolecules* **2005**, *38*, 8272.
[64] K. Wang, R. Li, J. H. Ma, Y. K. Jian, J. N. Che, *Green Chem.* **2016**, *18*, 476.
[65] C. D. Tran, T. M. Mututuvari, *Langmuir* **2015**, *31*, 1516.
[66] A. P. Manian, T. Pham, T. Bechtold, 10 - Regenerated Cellulosic Fibers, *Handbook of Properties of Textile and Technical Fibres*, 2, Woodhead Publishing, Cambridge, UK **2018**, pp. 329–343.
[67] J. Zhang, Y. Li, J. Li, Z. Zhao, X. Liu, Z. Li, Y. Han, J. Hu, A. Chen, *Powder Technol.* **2013**, *246*, 356.
[68] S. Sharma, A. Gupta, S. Mohd, S. T. Chik, C. Geek, B. M. Mistry, D. H. Kim, G. Sharma, *Int. J. Biol. Macromol.* **2017**, *104*, 189.
[69] H. J. Jin, D. L. Kaplan, *Nature* **2003**, *424*, 1057.
[70] Q. Lu, H. Zhu, C. Zhang, F. Zhang, B. Zhang, D. L. Kaplan, *Biomacromolecules* **2012**, *13*, 826.
[71] S. R. Koebley, D. Thorpe, P. Pang, P. Chrisochoides, I. Greving, F. Vollrath, H. C. Schniepp, *Biomacromolecules* **2015**, *16*, 2796.
[72] N. Goujon, X. Wang, R. Rajkowa, N. Byrne, *Chem. Commun.* **2012**, *48*, 1278.
[73] Y. Kajiura, S. Watanabe, T. Itou, K. Nakamura, A. Iida, K. Inoue, N. Yagi, Y. Shinohara, Y. Amemiya, *J. Struct. Biol.* **2006**, *155*, 438.
[74] L. Cera, G. M. Gonzalez, Q. Liu, S. Choi, C. O. Chantre, J. Lee, R. Gabardi, M. C. Choi, K. Shin, K. K. Parker, *Nat. Mater.* **2020**, *20*, 242.
[75] D. Qiao, W. Tu, L. Zhong, Z. Wang, B. Zhang, F. Jiang, *Polymer* **2019**, *11*, 1952.
[76] N. Li, Z. Cai, Y. Guo, T. Xu, D. Qiao, B. Zhang, S. Zhao, Q. Huang, M. Niu, C. Jia, L. Lin, Q. Lin, *Food Chem.* **2019**, *295*, 475.
[77] D. W. Litchfield, D. G. Baird, *Polymer* **2008**, *49*, 5027.
[78] S. C. Owen, D. P. Y. Chan, M. S. Shoichet, *Nano Today* **2012**, *7*, 53.
[79] D. R. Paul, *J. Appl. Polym. Sci.* **1968**, *12*, 383.
[80] N. Hameed, Q. Guo, *Cellulose* **2010**, *17*, 803.
[81] R. Hu, Y. Liu, S. Shin, S. Huang, X. Ren, W. Shu, J. Cheng, G. Tao, W. Xu, R. Chen, X. Luo, *Adv. Energy Mater.* **2020**, *10*, 1903921.
[82] M. van Elven, How Sustainable is Recycled Polyester?, https://fashionunited.uk/news/fashion/how-sustainable-is-recycled-polyester/2018111540000, (accessed: Aug, 2021).